

Analysis of the SBP-SAT Stabilization for Finite Element Methods

Part I: Linear problems

R. Abgrall[†], J. Nordström^{*}, P. Öffner^{*†}, and S. Tokareva[‡]

[†]Institute of Mathematics, University of Zurich, Switzerland

^{*}Department of Mathematics, Computational Mathematics, Linköping University, Sweden

[‡]Applied Mathematics and Plasma Physics Group, Los Alamos National Laboratory, USA

January 4, 2023

Abstract

A pure Galerkin scheme is notoriously unstable. To remedy this issue, stabilization terms are usually added and various formulations can be found in the literature. In this paper, we are also dealing with this problem, but present a different approach. We use the boundary conditions in our investigation in the sense that so called simultaneous approximation terms (SATs) are applied which are frequently used in the finite difference community. Here, the main idea is to impose the boundary conditions weakly. Specific boundary operators are constructed which guarantee stability. The SAT approach has already been used in the discontinuous Galerkin framework, but here we apply it -up to our knowledge- for the first time together with a continuous Galerkin scheme. We demonstrate that a pure continuous Galerkin scheme is stable if the boundary conditions are implemented in the correct way. This contradicts the general perception of stability problems for pure Galerkin schemes. In numerical simulations, we verify our theoretical analysis.

1 Introduction

In recent years, significant efforts have been made to construct and develop high-order methods for the solution of hyperbolic balance laws, and most of the common methods are either based on finite difference (FD) or finite element (FE) approaches. In the FE framework, one favorable, if not the most favorable scheme, seems to be the discontinuous Galerkin (DG) method introduced by Reed and Hill [1] because of its good stability properties [2, 3, 4, 5]. In the stability proofs, so called summation-by-parts (SBP) operators are used [6, 7, 8, 9, 5, 10]. SBP operators originate in the FD framework [11] and lead to a way to demonstrate stability similar to the one in the continuous analysis [12, 13, 14]. Together with SBP operators, Simultaneous Approximation Terms (SATs) that impose the boundary conditions weak are applied. The SBP-SAT technique is powerful and universally applicable. Certainly, one of the reasons for the popularity of DG is that the numerical solution is allowed to have discontinuities at the element boundaries, and, since non-linear hyperbolic problems are supporting shocks (like Riemann problems), this property is believed to be desirable. Another reason, maybe the most important, is that DG methods leads to block diagonal mass matrices which are easy to invert.

The difference between a DG approach and continuous Galerkin (CG), besides the structure of the mass matrix, is that in CG the approximated solution is forced to be continuous also over the element boundaries and this restriction seems to be quite strong also in terms of stability where a common belief in the research

^{*}Corresponding author: P. Öffner, philipp.oeffner@math.uzh.ch

community is that a pure CG scheme is notoriously unstable¹. Therefore, stabilization terms have been developed and are frequently applied to remedy this issue [15, 16, 17]. Even there exist some preliminary stability results [18, 19, 20] including the procedure at the boundary where the main idea is to switch the norm of the trial space. However, these results may seem forgotten in the community.

In this paper, we also focus on the stability property of a pure Galerkin scheme, but follow a different approach. Our preliminary idea/thought is: If one considers the DG method with one element, the method is stable through the investigation done in the literature mentioned above. There is nothing that says that the approximation space must be a broken polynomial space, the only thing that is needed is that the trial and test function must have some kind of regularity within the elements, so that the divergence theorem (or SBP techniques) can be applied. Continuity is enough. Hence, one can see a CG method as a DG one, with only one element (the union of the simplex) with an approximation space made of polynomials with continuity requirement between the simplex. Hence, what is the difference between these two approaches? The answer to this question points to the procedure at the boundary.

In the stability proofs, the usage of SATs is essential. However, up-to-our-knowledge SATs have never been used together with a pure CG scheme and this is the topic of this paper. We divide the paper as follows: In the second section, we shortly introduce the continuous Galerkin scheme which is used and investigated in the following. Next, we introduce and repeat the main idea of the SAT procedure from the FD framework and extend it to the Galerkin approach. We show that the determination of the boundary operators is essential. In section 4, we focus on the eigenvalue analysis of the spatial operators and derive conditions from the continuous setting to build adequate boundary operators in the discrete framework. We give some recipes which will be used in section 5 to support our analysis in numerical experiments. Finally, we conclude and discuss future work.

2 Continuous Galerkin Scheme

In this section, we shortly introduce the pure continuous Galerkin scheme (CG) as it is also known in the literature [21, 16, 11]. We are interested in the numerical approximation of a hyperbolic problem

$$\frac{\partial U}{\partial t} + \operatorname{div} f(U) = 0 \quad (1)$$

with suitable initial and boundary conditions. Later, we will focus on the boundary condition, but for the explanation of CG this is not important. The domain Ω is split into subdomains Ω_h (e.g triangles/quads in two dimensions, tetrahedrons/hex in 3D). We denote by K the generic element of the mesh and by h the characteristic mesh size. Then, the degrees of freedom (DoFs) σ are defined in each K : we have a set of linear forms acting on the set \mathbb{P}^k of polynomials of degree k such that the linear mapping $q \in \mathbb{P}^k \mapsto (\sigma_1(q), \dots, \sigma_{|\Sigma_K|}(q))$ is one-to-one. The set \mathcal{S} denote the set of degrees of freedom in all elements. The solution U will be approximated by some element from the space \mathcal{V}^h defined by

$$\mathcal{V}^h := \bigoplus_K \{U^h \in \mathcal{L}^2(K), U^h|_K \in \mathbb{P}^k\} \cap C^0(\Omega). \quad (2)$$

A linear combination of basis functions $\varphi_\sigma \in \mathcal{V}^h$ will be used to describe the numerical solution

$$U^h(x) = \sum_{K \in \Omega_h} \sum_{\sigma \in K} U_\sigma^h \varphi_\sigma|_K(x), \quad \forall x \in \Omega \quad (3)$$

As basis functions we are working either with Lagrange interpolation where the degrees of freedom are associated to points in K or Bézier polynomials.

To start the discretisation, we apply a Galerkin approach and multiply with a test function V^h and integrate over the domain. This gives

$$\int_\Omega (V^h)^T \frac{\partial U}{\partial t} dx + \int_\Omega (V^h)^T \operatorname{div} f(U) dx = 0. \quad (4)$$

¹We like to mention that also parts of the authors had this belief before starting the project.

Using the divergence theorem, we get

$$\int_{\Omega} (V^h)^T \frac{\partial U}{\partial t} dx - \int_{\Omega} (\nabla V^h)^T f(U) dx + \int_{\partial\Omega} (V^h)^T f(U) \cdot \mathbf{n} d\gamma = 0. \quad (5)$$

By choosing $V^h = \varphi_{\sigma}$ for any $\sigma \in \mathcal{S}$ and inserting (3), we obtain a system of equations:

$$\sum_{K \in \Omega_h} \sum_{\sigma' \in K} \left(\frac{\partial U_{\sigma'}^h(t)}{\partial t} \int_K \varphi_{\sigma'}(x) \varphi_{\sigma}(x) dx - \int_K \nabla \varphi_{\sigma'}(x) f(U^h) dx \right) = 0, \quad (6)$$

that in practice we compute using a quadrature rule:

$$\sum_{K \in \Omega_h} \sum_{\sigma' \in K} \left(\frac{\partial U_{\sigma'}^h(t)}{\partial t} \oint_K \varphi_{\sigma'}(x) \varphi_{\sigma}(x) dx - \oint_K \nabla \varphi_{\sigma'}(x) f(U^h) dx \right) = 0,$$

where \oint represents the quadrature rules for the volume and surface integrals.

In this paper, we are considering only linear problems, i.e. the flux is linear in U , but may depend on the spatial coordinate. In all the numerical experiences, we will make the spatial dependency simple enough (i.e. typically polynomial in x), so that it will always be possible to find a standard quadrature formula that make the formula *exact*. In other words, in this paper we proceed such that (6) is always exactly reproduced, unless it is specified.

Using a matrix formulation, we obtain the classical FE framework:

$$\underline{\underline{M}} \frac{\partial}{\partial t} \underline{U}^h + \underline{\underline{F}} = 0 \quad (7)$$

where \underline{U}^h denotes the vector of degrees of freedom, $\underline{\underline{F}}$ is the approximation of $\text{div } f$ and $\underline{\underline{M}}$ is a mass matrix². In case of continuous elements, this matrix is sparse but not block diagonal, contrary to the discontinuous Galerkin methods. It is well-known that the continuous Galerkin scheme suffers from stability issues. Therefore, it is common to add stabilization terms to the scheme as for example in [17]. However, we follow a different approach in this paper and will renounce these classical stabilisation techniques. In order to do this, we need more known results from the literature, which we will briefly repeat here.

3 Weak Boundary Conditions

3.1 SATs in SBP-FD framework

Weak boundary conditions implemented using simultaneous approximation terms (SATs) was originally developed in the finite difference (FD) framework. Together with summation-by-parts (SBP) operators it provides a powerful tool for proofs of semidiscrete (L_2) stability of linear problems by the energy method, see [14, 12, 23] for details.

Here, we present a short introductory example of the SBP-SAT technique as it presented [22, 14]. Consider the linear advection equation

$$\begin{aligned} \frac{\partial u}{\partial t} + a \frac{\partial u}{\partial x} &= 0, \quad 0 \leq x \leq 1, \quad t > 0, \\ u(x, 0) &= u_{in}(x), \\ u(x, t) &= b(x, t) \text{ for inflow boundary} \end{aligned} \quad (8)$$

where u_{in} is the initial condition and b is the boundary data in L^2 that is only define on the inflow part of $\partial[0, 1] = \{0, 1\}$. In other words, if $a > 0$, the b is only set for $x = 0$, and if $a < 0$, this will be for $x = 1$ only.

²In the finite difference community $\underline{\underline{M}}$ is called norm matrix and is classically abbreviated with P , c.f. [14, 22].

A semi-discretisation of (8) is given in terms of SBP operators.

$$\begin{aligned} \frac{\partial \underline{u}}{\partial t} + a \underline{D} \underline{u} &= \underline{M}^{-1} \underline{\mathbb{S}}, \quad t > 0, \\ \underline{u}(0) &= \underline{u}_{in}, \end{aligned} \quad (9)$$

with $\underline{u} = (u_0, u_1, \dots, u_N(t))^T$ are the coefficients of u and similarly for \underline{u}_{in} . The coefficients correspond to the degrees of freedom in the finite element setting and are used to express the numerical solution (3) in the grid points. \underline{M} is a symmetric positive definite mass matrix which approximates the usual L^2 scalar product. The term \underline{D} is a difference matrix. This is exemplified below as

$$\underline{D} \underline{u} \approx \frac{\partial}{\partial x} u \text{ and } \|\underline{u}\|_{\underline{M}}^2 := \underline{u}^T \underline{M} \underline{u} \approx \int_0^1 u^2(x) dx. \quad (10)$$

Instead of having an extra equation on the boundary like in (8), the boundary condition is enforced weakly by the term $\underline{\mathbb{S}} = (\mathbb{S}_0, 0, \dots, \mathbb{S}_N)^T$ which is called the SAT. We will focus on this operator more precisely and demonstrate how it should be selected to guarantee stability for (9).

Definition 3.1. *The scheme (9) is called strongly energy stable if*

$$\|\underline{u}(t)\|_{\underline{M}}^2 \leq K(t) \left(\|\underline{u}_{in}\|_{\underline{M}}^2 + \max_{t_1 \in [0, t]} \|b_0(t_1)\|^2 \right) \quad (11)$$

holds. The term $K(t)$ is bounded for any finite t and independent from u_{in} , b_0 and the mesh.

Remark 3.2. *The definition 3.1 is formulated in terms of the initial value problem (8) where only one boundary term is fixed. Indeed, extensions are straightforward. If an additional forcing function is considered at the right hand side of (8), we have to include the maximum of this function in (11) in the spirit of b_0 , for details see [14].*

As established in [24], we can prove the following:

Proposition 3.3. *Let $\underline{D} = \underline{M}^{-1} \underline{Q}$ be an SBP operator with \underline{Q} that fulfills*

$$\underline{Q} + \underline{Q}^T = \underline{B} = \text{diag}(-1, 0, \dots, 0, 1). \quad (12)$$

Let $a^+ = \max\{a, 0\}$ and $a^- = \min\{a, 0\}$, $b_0 = b(0, t)$ and $b_N = b(1, t)$. If $\mathbb{S}_0 = \tau_0 a^+(u_0 - b_0)$ with $\tau_0 \leq -\frac{1}{2}$, and $\mathbb{S}_N = \tau_N a^-(u_N - b_N)$ with $\tau_N \leq -\frac{1}{2}$ then the scheme (9) is energy stable.

Proof. Multiplying (9) with $\underline{u}^T \underline{M}$ yields

$$\underline{u}^T \underline{M} \frac{\partial}{\partial t} \underline{u} + a \underline{u}^T \underline{M} \underline{D} \underline{u} = \underline{u}^T \underline{\mathbb{S}}. \quad (13)$$

Transpose (13) and adding both equations together leads to

$$\frac{d}{dt} \|\underline{u}\|_{\underline{M}}^2 = \underline{u}^T \underline{M} \frac{\partial}{\partial t} \underline{u} + \frac{\partial}{\partial t} \underline{u}^T \underline{M} \underline{u} = -a \underline{u}^T (\underline{Q} + \underline{Q}^T) \underline{u} + 2 \underline{u}^T \underline{\mathbb{S}}.$$

Further, we obtain from (12)

$$\frac{d}{dt} \|\underline{u}\|_{\underline{M}}^2 = \left(a u_0^2 + 2a^+ \tau u_0 (u_0 - b_0) \right) - \left(a u_N^2 - 2a^- \tau u_N (u_N - b_N) \right).$$

Looking at the cases $a > 0$ and $a < 0$, if $\tau_0, \tau_N < -\frac{1}{2}$, we find

$$\frac{d}{dt} \|\underline{u}\|_{\underline{M}}^2 \leq -\frac{a^+ \tau^2}{(1 + 2\tau)} b_0^2 + \frac{a^- \tau^2}{(1 + 2\tau)} b_N^2 \leq 0.$$

□

This shows that boundary operator \mathbb{S} can be chosen in such way that it guarantees stability for the SBP-SAT approximation of (8). Next, we will apply this technique in the Galerkin framework.

3.2 SATs in the Galerkin-Framework

Instead of working with SBP-FD framework we consider now for the approximation of (8), a Galerkin approach. In [6, 5] it is presented that also the discontinuous Galerkin spectral element method satisfies a discrete summation-by-parts (SBP) property and can be interpreted as an SBP-SAT scheme with diagonal mass matrix. As we described already in section 2, the differences between the continuous and discontinuous Galerkin approach are the solution space (2) and structure of the mass matrix (7) which is not block diagonal in CG. However, the approach with SAT terms can still be used to ensure stability also in case of CG but one has to be precise, as we will explain in the following.

Let us step back to the proof of Proposition 3.3 and have a closer look on it. Essential in the proof is condition (12). Let us focus on this condition for a FE based discretisation of (8) as described also in [22]. We approximate (8) now with $u^h(x, t) = \sum_{j=0}^N u_j^h(t) \varphi_j(x)$ where φ_j are basis functions and u_j^h are the coefficients. Let us assume that φ_j are Lagrange polynomials where the degrees of freedoms are associated to points in the interval. Introducing the scalar product

$$\langle u, v \rangle = \int_I u(x) v(x) dx,$$

let us consider the variational formulation of (8) with test function φ_i and inserting the approximation yields

$$\left\langle \frac{\partial}{\partial t} u^h(t, x), \varphi_i(x) \right\rangle + \left\langle a \frac{\partial}{\partial x} u^h(t, x), \varphi_i(x) \right\rangle = 0, \quad \forall i = 0, \dots, N$$

i.e.

$$\int_I \sum_{j=0}^N \left(\frac{\partial}{\partial t} u_j^h(t) \right) \varphi_j(x) \varphi_i(x) dx + a \int_I \sum_{j=0}^N u_j^h(t) \left(\frac{\partial}{\partial x} \varphi_j(x) \right) \varphi_i(x) dx = 0.$$

and finally

$$\sum_{j=0}^N M_{i,j} \left(\frac{\partial}{\partial t} u_j^h(t) \right) + a \sum_{j=0}^N Q_{i,j} u_j^h(t) = 0 \quad (14)$$

where

$$M_{i,j} = \int_I \varphi_j(x) \varphi_i(x) dx \quad \text{and} \quad Q_{i,j} = \int_I \left(\frac{\partial}{\partial x} \varphi_j(x) \right) \varphi_i(x) dx. \quad (15)$$

In matrix formulation (14) can be written

$$\underline{\underline{M}} \frac{\partial}{\partial t} \underline{u} + a \underline{\underline{Q}} \underline{u} = 0$$

as it is also described in [22]. Let us check (12). Therefore, we consider

$$\begin{aligned} Q_{i,j} + Q_{i,j}^T &= \int_I \left(\frac{\partial}{\partial x} \varphi_j(x) \right) \varphi_i(x) dx + \left(\frac{\partial}{\partial x} \varphi_i(x) \right) \varphi_j(x) dx = \int_I \frac{\partial}{\partial x} (\varphi_j(x) \varphi_i(x)) dx \\ &= \varphi_i(x) \varphi_j(x) \Big|_0^1 = \varphi_i(1) \varphi_j(1) - \varphi_i(0) \varphi_j(0) \quad \forall i, j = 0, \dots, N. \end{aligned} \quad (16)$$

If the boundaries are included in the set of degrees of freedom, then we obtain

$$\varphi_i(1) \varphi_j(1) - \varphi_i(0) \varphi_j(0) = \begin{cases} 1 & \text{for } i = j = N, \\ -1 & \text{for } i = j = 0, \\ 0 & \text{elsewhere.} \end{cases}$$

Up to this point exact integrals are considered but the same steps are valid if a quadrature rule is applied with sufficient accuracy, especially (16) has to hold exactly. If this is the case, we can apply the proof of proposition 3.3 and demonstrate:

Proposition 3.4. *If the Galerkin method described above together with a SAT approach is applied to (8). If $\mathbb{S} = \tau a^+(u_0 - b_0)\delta_{x=0} + \tau a^-(u_N - b_N)\delta_{x=x_N=1}$ with $\tau \leq -\frac{1}{2}$ is used then the described scheme is energy stable. The weak formulation of the problem writes:*

$$\left\langle \frac{\partial}{\partial t} u^h(t, x), \varphi_i(x) \right\rangle + \left\langle a \frac{\partial}{\partial x} u^h(t, x), \varphi_i(x) \right\rangle = \tau a^+(u^h(0, t) - b_0^h(t))\varphi_i(0) + \tau a^-(u^h(1, t) - b_N)\varphi_i(1) = 0, \quad \forall i, \dots, N$$

Proof. For simplicity, we consider the case $a > 0$ only.

The SAT techniques adds a penalty term into the approximation (8) on the right side. We focus now on the energy. Therefore, we multiply also with u^h instead of φ_i and rearrange the terms. We obtain for the semi-discretization (14):

$$\sum_{i,j=0}^N M_{i,j} \left(\frac{\partial}{\partial t} u_j^h(t) \right) u_i^h(t) + a \sum_{i,j=0}^N Q_{i,j} u_j^h(t) u_i^h(t) = 2a\tau u_0^h(t)(u_0^h(t) - b_0(t))$$

where we used the fact that $u^h(t, 0) = \sum_{i=0}^N u_i^h(t)\varphi_i(0) = u_0^h(t)$ is valid. By following the steps of the proof of proposition 3.3 and using the above considerations we get the final result. \square

In the derivation above, we restricted ourselves to one-dimensional problems using Lagrange interpolations. Nevertheless, this shows that a continuous Galerkin method is stable if the boundary condition is enforced by a proper penalty term. For the general FE semi-discretization of (7) it is straightforward to the procedure. For a general linear problem (scalar or systems) the formulation (7)³ can be written with penalty terms as

$$\underline{\underline{M}} \frac{\partial}{\partial t} \underline{\underline{U}}^h + \underline{\underline{Q}}_1 \underline{\underline{A}} \underline{\underline{U}}^h = \alpha \Pi \left(\underline{\underline{U}}^h \right) \quad (17)$$

where Π is the boundary operator which includes the boundary conditions. $\underline{\underline{A}} \underline{\underline{U}}^h$ represents the flux and $\underline{\underline{Q}}_1$ the spatial operator. The matrix Π is usually sparse and we can formulate the following.

Theorem 3.5. *Apply the general FE semidiscretization (17) together with the SAT approach to a linear equation and let the mass matrix $\underline{\underline{M}}$ of (17) be symmetric. If the boundary operator $\alpha \Pi$ together with the discretization $\underline{\underline{Q}}_1$ can be chosen such that*

$$(\alpha \Pi - \underline{\underline{Q}}_1 \underline{\underline{A}}) + \left(\alpha \Pi - \underline{\underline{Q}}_1 \underline{\underline{A}} \right)^T \quad (18)$$

has only non-positive eigenvalues $\underline{\underline{\Delta}}$, then the scheme is energy stable.

Proof. We use the energy approach and multiply our discretization with $\underline{\underline{U}}^h$ instead of φ_i and add the transposed equation using $\underline{\underline{M}}^T = \underline{\underline{M}}$. We obtain

$$\frac{d}{dt} \|\underline{\underline{U}}^h\|_{\underline{\underline{M}}}^2 = \underline{\underline{U}}^{h,T} \left((\alpha \Pi - \underline{\underline{Q}}_1 \underline{\underline{A}}) + \left(\alpha \Pi - \underline{\underline{Q}}_1 \underline{\underline{A}} \right)^T \right) \underline{\underline{U}}^h = \underline{\underline{W}}^{h,T} \underline{\underline{\Delta}} \underline{\underline{W}}^h \leq 0.$$

\square

Remark 3.6. *This theorem yields directly conditions for a FE based stable scheme. If (18) is not fulfilled, stabilization terms have to be added. **However, no internal stabilization terms are necessary when (16) holds.** For this result to hold, a number of requirements are needed. The distribution of the degrees of freedom should be suitable for the problem and the mesh and the quadrature rule must be chosen to guarantee exactness of all the calculations. In the numerical test, we will present an example of what happens if the quadrature rule is not sufficiently exact.*

³Remember that the flux is linear with Jacobian A .

Furthermore, in case of a non-conservative formulation of the hyperbolic problem or in case of variable coefficients a skew-symmetric formulation must be applied in the way as it is described in [22, 25, 26]. If the implementation of the continuous Galerkin method is done in such way that the condition (18) are fulfilled, then by applying the SAT technique the method is stable only through our boundary conditions. To our opinion, this is **contrary** to common belief about continuous Galerkin methods. The only stabilizing factor needed is a proper implementation of boundary conditions. For the linear scalar case, the proof is given in (3.4). In the following, we will extend this theory to more general cases.

4 Estimation of the SAT-Boundary Operator

As described before, a proper implementation of the boundary condition is essential for stability. Here, we give a recipe how these SAT boundary operators can be chosen to get a stable CG scheme for different types of problems.

First, we are considering a scalar equation in 2D and transfer the eigenvalue analysis for the spatial operator from the continuous to the discrete setting. Then, we extend our investigation to 1D systems. Using again the continuous setting, we develop estimations for Π and transfer the results to the finite element framework. Finally, we extend the investigation to the system case in two dimensions which will also be used in the numerical section later.

4.1 Eigenvalue Analysis

In the following part, we derive the conditions on the boundary operators and perform an eigenvalue analysis to get well posedness in the continuous setting. Next, the results are transformed to the discrete framework to guarantee stability of the discrete scheme.

4.1.1 The scalar case

Continuous Setting

Consider the initial boundary value problem

$$\begin{aligned} \frac{\partial}{\partial t}u + a\frac{\partial}{\partial x}u + b\frac{\partial}{\partial y}u &= 0 & x \in \Omega, \quad t > 0, \\ Bu &= g & x \in \partial\Omega, \quad t > 0, \\ u &= f & x \in \Omega, \quad t = 0. \end{aligned} \tag{19}$$

Without loss of generality, it is enough to consider the homogeneous boundary conditions and we consider the spatial operator

$$Du := \left(a\frac{\partial}{\partial x} + b\frac{\partial}{\partial y} \right) u, \tag{20}$$

considered in the subspace of functions for which $Bu = 0$. This operator will be dissipative if $\langle u, Du \rangle > 0$. Using the Gauss-Green theorem, we obtain

$$\langle u, Du \rangle = \int_{\Omega} u Du \, d\Omega = \int_{\partial\Omega} \frac{a}{2} u^2 dy - \frac{b}{2} u^2 dx = \int_{\partial\Omega} \underbrace{(a, b) \cdot \mathbf{n}}_{:=a_n} u^2 ds. \tag{21}$$

The operator will be dissipative if $\int_{\partial\Omega} a_n u^2 ds > 0$. Looking at this question amounts to looking at the spectral properties of the operator D . The question rises: How do we guarantee this condition? This is the role of the boundary conditions, i.e. when $a_n \leq 0$, we need to impose $u = 0$. For outflow, i.e. $\partial\Omega_{out}$ we get $a_n > 0$ and using this information, we directly obtain

$$\langle u, Du \rangle = \int_{\partial\Omega_{out}} a_n u^2 ds > 0. \tag{22}$$

We do not go further into details about well posedness, but we recommend [23, 27, 28] for details. Now, we transfer our analysis to the discrete framework and imitate this behavior discretely.

Discrete Setting

We have to approximate the spatial operator D and the boundary condition (B.C), i.e. $Du + B.C$ which is approximated an operator of the form $\underline{\underline{M}}^{-1}(\underline{\underline{Q}} - \alpha\Pi)\underline{\underline{u}}$. The term $\underline{\underline{M}}^{-1}\underline{\underline{Q}}\underline{\underline{u}}$ approximates Du where $\alpha\Pi\underline{\underline{u}}$ is used to describe Bu weakly. $\underline{\underline{M}}$ denotes the mass matrix⁴ and $\underline{\underline{M}}^{-1}\underline{\underline{Q}}$ the derivative matrix, in the context of SBP [14]. Here, the projection operator Π works at the boundary points. Looking at the dissipative nature of $\underline{\underline{M}}^{-1}\underline{\underline{Q}}\underline{\underline{u}}$ amounts to study its spectrum. The eigenvalue problem is

$$\underline{\underline{M}}^{-1}(\underline{\underline{Q}} - \alpha\Pi)\underline{\underline{u}} = \lambda\underline{\underline{u}} \quad (23)$$

We denote by $\underline{\underline{u}}^{*,T}$, the adjoint of $\underline{\underline{u}}$, multiply with $\underline{\underline{u}}^{*,T}\underline{\underline{M}}$ and obtain

$$\underline{\underline{u}}^{*,T}(\underline{\underline{Q}} - \alpha\Pi)\underline{\underline{u}} = \lambda\underline{\underline{u}}^{*,T}\underline{\underline{M}}\underline{\underline{u}} = \lambda\|\underline{\underline{u}}\|_M^2. \quad (24)$$

We transpose (24) and add both equations together. This results in

$$\underbrace{\underline{\underline{u}}^{*,T} \left((\underline{\underline{Q}} + \underline{\underline{Q}}^T) - \alpha(\Pi + \Pi^T) \right) \underline{\underline{u}}}_{:=BT} = 2\operatorname{Re}(\lambda)\|\underline{\underline{u}}\|_M^2. \quad (25)$$

The boundary terms (BT) correspond to $\int_{\partial\Omega_{out}} a_n u^2 ds$ with a properly chosen Π . The matrix

$$\left(\alpha(\Pi + \Pi^T) - (\underline{\underline{Q}} + \underline{\underline{Q}}^T) \right) \geq 0$$

is positive semi-definite. However, the remaining terms in the boundary term makes $\operatorname{Re}(\lambda) > 0$, i.e. the eigenvalues for the spatial operator have a strictly positive real parts only.

Next, we estimates the boundary operators such that theorem 3.5 is fulfilled and a pure CG scheme is stable. We start with the continuous energy analysis and derive the estimate above. Afterwards, we translate the result to the discrete FE framework as done for the scalar one-dimensional case.

4.1.2 Continuous Energy Analysis for 1D Systems

First, we extend our result to the 1D system case. The problem under consideration is given by:

$$\begin{aligned} \frac{\partial U}{\partial t} + A \frac{\partial U}{\partial x} &= 0, & x \in (0, 1), \\ L_0(U) &= g_0(t), & x = 0, \\ L_1(U) &= g_1(t), & x = 1, \\ U(x, 0) &= U_0(x), & x \in [0, 1], \end{aligned} \quad (26)$$

where A is a $n \times n$ symmetric matrix, and we assume L_0 and L_1 to be linear. If n_0 is the number of incoming characteristics at $x = 0$ and n_1 the number of incoming characteristics at $x = 1$, we know that the rank of L_0 (resp L_1) is n_0 (resp n_1). The system (26) admits an energy: if we multiply $\frac{\partial U}{\partial t} + A \frac{\partial U}{\partial x} = 0$ by U^T , we first get

$$\int_0^1 U^T \frac{\partial U}{\partial t} dx + \int_0^1 U^T A \frac{\partial U}{\partial x} dx = 0.$$

⁴In the finite difference context this matrix is also called norm matrix.

The energy $E = \frac{1}{2} \int_0^1 U^2 dx$ satisfies

$$\frac{dE}{dt} + U(1, t)^T A_n U(1, t) - U(0, t)^T A_n U(0, t) = 0.$$

To understand the role of boundary conditions, we follow what is usually done for conservation laws, we consider the weak form of (26): let φ be a regular vector function in space and time. We multiply the equation by φ^T , integrate and get:

$$\int_0^T \int_0^1 \varphi^T \frac{\partial U}{\partial t} dx dt - \int_0^T \int_0^1 \frac{\partial \varphi^T}{\partial x} AU dx dt + \int_0^T \varphi(1, t)^T A_n U(1, t) dt - \int_0^T \varphi(0, t)^T A_n U(0, t) dt = 0$$

In order to enforce the boundary conditions weakly, we modify this relation by:

$$\begin{aligned} \int_0^T \int_0^1 \varphi^T \frac{\partial U}{\partial t} dx dt - \int_0^T \int_0^1 \frac{\partial \varphi^T}{\partial x} AU dx dt \\ + \int_0^T \varphi(1, t)^T A_n U(1, t) dt - \int_0^T \varphi(0, t)^T A_n U(0, t) dt \\ = \int_0^T \varphi(1, t)^T \Pi_1 (L_1(U) - g_1) dt - \int_0^T \varphi(0, t)^T \Pi_0 (L_0(U) - g_0) dt. \end{aligned} \quad (27)$$

The operators Π_0 and Π_1 are selected in such a way that

1. For any t , the image of the boundary operator L_0 is the same as the image of $\Pi_0 L_0$, i.e. there is no loss of boundary information, and the same applies for Π_1 and L_1 .
2. If $\varphi = U$, then

$$\frac{dE}{dt} < 0.$$

A solution to this problem is given by the following: First, let $A = X \Lambda X^T$ where Λ are the eigenvalues of A and X is the matrix which rows are the right eigenvectors of A . Secondly, we have $X^T X = \mathbb{I}$ and choose:

$$\Pi_0 (L_0(U) - g_0) = X \Lambda^- \begin{pmatrix} R_0 \\ \mathbf{0}_{n-n_0} \end{pmatrix} X^T - \begin{pmatrix} g_0 \\ \mathbf{0}_{n-n_0} \end{pmatrix}, \text{ and } \Pi_1 (L_1(U) - g_1) = X \Lambda^- \begin{pmatrix} R_1 \\ \mathbf{0}_{n-n_1} \end{pmatrix} X^T - \begin{pmatrix} g_1 \\ \mathbf{0}_{n-n_1} \end{pmatrix}. \quad (28)$$

where Λ^- are the negative eigenvalues only. Here we have introduced the operator R_0 and R_1 which are just L_0 and L_1 written using characteristic variables, and not U . We will write

$$\Pi(L(U) - g) = (L_0(U) - g_0) \delta_{x=0} + (L_1(U) - g_1) \delta_{x=1}$$

in the sequel.

Step 1: Strong Implementation

First, we consider again the strong implementation of the problem.

$$\frac{d}{dt} \|U\|^2 = U^T AU \Big|_{x=0} - U^T AU \Big|_{x=1}$$

For simplicity, we look only at what occurs for $x = 0$. Let $A = X \Lambda X^T$ where Λ are the eigenvalues of A and X is the matrix which rows are the right eigenvectors of A . Then, we obtain

$$U^T AU = U^T X \Lambda X^T U = (X^T U)^T \Lambda (X^T U) = \begin{pmatrix} W^+ \\ W^- \end{pmatrix}^T \begin{pmatrix} \Lambda^+ & 0 \\ 0 & \Lambda^- \end{pmatrix} \begin{pmatrix} W^+ \\ W^- \end{pmatrix} \quad (29)$$

with $W^+ = (X^T U)^+$ are the ingoing waves and they have the size of the positive eigenvalues Λ^+ . Analogously, $W^- = (X^T U)^-$ are the outgoing waves with size of Λ^- . A general homogeneous boundary condition is $W^+ = RW^-$, since with that form we get

$$U^T A U = (W^-)^T (\Lambda^- + R^T \Lambda^+ R) W^- \leq 0 \quad (30)$$

if the matrix in the bracket is negative semidefinite.

Step 2: Weak Implementation

Assume now that we have chosen an R such that

$$\Lambda^- + R^T \Lambda^+ R \leq 0. \quad (31)$$

The energy is given (remember $\partial\Omega = \{0, 1\}$)

$$\int_{\Omega} U^T \frac{\partial U}{\partial t} dx + \int_{\Omega} U^T A \frac{\partial U}{\partial x} dx = \int_{\partial\Omega} U^T \Pi (W^+ - RW^-) dx \quad (32)$$

Second, we consider everything at the boundary

$$\frac{1}{2} \frac{d}{dt} \|U\|^2 = -\frac{1}{2} \int_{\partial\Omega} U^T A U dx + \int_{\partial\Omega} U^T \Pi (W^+ - RW^-) dx + \int_{\partial\Omega} (W^+ - RW^-)^T \Pi^T U dx \quad (33)$$

Since $\int_{\partial\Omega} = \int_{x=0} + \int_{x=1}$, we focus only on the $x = 0$ part. We define $\tilde{\Pi}$ such that $U^T \Pi = (W^+)^T \tilde{\Pi}$ and get for the integrands

$$W^+ \Lambda^+ W^+ + W^- \Lambda^- W^- + (W^+)^T \tilde{\Pi} (W^+ - RW^-) + (W^+ - RW^-)^T \tilde{\Pi}^T W^+ \quad (34)$$

Collecting the terms, we obtain

$$\begin{pmatrix} W^+ \\ W^- \end{pmatrix}^T \underbrace{\begin{pmatrix} \Lambda^+ + \tilde{\Pi} + \tilde{\Pi}^T & -\tilde{\Pi} R \\ -R^T \tilde{\Pi}^T & \Lambda^- \end{pmatrix}}_{=:WB} \begin{pmatrix} W^+ \\ W^- \end{pmatrix} \quad (35)$$

We must select $\tilde{\Pi}$ such that the matrix WB is negative definite. Now, let us use the fact that we have the strong condition (31). By adding and subtracting, we obtain

$$\underbrace{\begin{pmatrix} W^+ \\ W^- \end{pmatrix}^T \begin{pmatrix} \Lambda^+ + \tilde{\Pi} + \tilde{\Pi}^T & -\tilde{\Pi} R \\ -R^T \tilde{\Pi}^T & -R^T \Lambda^+ R \end{pmatrix} \begin{pmatrix} W^+ \\ W^- \end{pmatrix}}_{=:Q} + \underbrace{W^- (\Lambda^- + R^T \Lambda^+ R) W^-}_{\leq 0 \text{ by (31)}} \quad (36)$$

We re-order Q :

$$Q = \begin{pmatrix} W^+ \\ RW^- \end{pmatrix}^T \begin{pmatrix} \Lambda^+ + \tilde{\Pi} + \tilde{\Pi}^T & -\tilde{\Pi} \\ -\tilde{\Pi}^T & -\Lambda^+ \end{pmatrix} \begin{pmatrix} W^+ \\ RW^- \end{pmatrix}$$

We choose $\tilde{\Pi} = \alpha \Lambda^+$ with α scalar and get

$$Q = \begin{pmatrix} W^+ \\ RW^- \end{pmatrix}^T \begin{pmatrix} \Lambda^+(1+2\alpha) & -\Lambda^+ \\ -\Lambda^+ & -\Lambda^+ \end{pmatrix} \begin{pmatrix} W^+ \\ RW^- \end{pmatrix} = \begin{pmatrix} W^+ \\ RW^- \end{pmatrix}^T \begin{pmatrix} (1+2\alpha) & -1 \\ -1 & -1 \end{pmatrix} \otimes \underbrace{\Lambda^+}_{>0} \begin{pmatrix} W^+ \\ RW^- \end{pmatrix}$$

We choose α such that the matrix is negative semidefinite. With $\alpha = -1$, it is

$$Q = - \begin{pmatrix} W^+ \\ RW^- \end{pmatrix}^T \underbrace{\begin{pmatrix} 1 & 1 \\ 1 & 1 \end{pmatrix}}_{=:G} \otimes \Lambda^+ \begin{pmatrix} W^+ \\ RW^- \end{pmatrix}$$

G has the eigenvalues 0 and 2 and we obtain stability thanks to (36) and (31).

4.1.3 Extension to 2D Symmetric Systems

Next, we will extend our investigation to the general hyperbolic system

$$\begin{aligned} \frac{\partial U}{\partial t} + A \frac{\partial U}{\partial x} + B \frac{\partial U}{\partial y} &= 0, \quad (x, y) \in \Omega, t > 0 \\ L_{\mathbf{n}} U &= G_{\mathbf{n}} \quad (x, y) \in \partial\Omega, t > 0 \end{aligned} \quad (37)$$

where $A, B \in \mathbb{R}^{m \times n}$ are the Jacobian matrices of the system, the matrix $L_{\mathbf{n}} \in \mathbb{R}^{q \times m}$ and the vector $G_{\mathbf{n}} \in \mathbb{R}^q$ are known, \mathbf{n} is the local outward unit vector, q is the number of boundary conditions to satisfy. We assume that A, B are constant and the system (37) is symmetrizable. It exists a symmetric and invertible matrix P such that for any vector $\mathbf{n} = (n_x, n_y)^T$ the matrix

$$B_{\mathbf{n}} = A_{\mathbf{n}} P$$

is symmetric with $A_{\mathbf{n}} = A n_x + B n_y$. Using the matrix P , one can introduce new variables $V = P^{-1/2} U$. The original variable can be expressed as $U = P^{1/2} V$ and the original system (37) will become

$$P^{1/2} \frac{\partial V}{\partial t} + A P^{1/2} \frac{\partial V}{\partial x} + B P^{1/2} \frac{\partial V}{\partial y} = 0. \quad (38)$$

Multiplying (38) from the left by $P^{-1/2}$ we obtain the system

$$\frac{\partial V}{\partial t} + P^{-1/2} A P^{1/2} \frac{\partial V}{\partial x} + P^{-1/2} B P^{1/2} \frac{\partial V}{\partial y} = 0. \quad (39)$$

which is symmetric since $P^{-1/2} A P^{1/2} n_x + P^{-1/2} B P^{1/2} n_y = P^{-1/2} B_{\mathbf{n}} P^{-1/2}$. Focusing on the boundary treatment of the problem and using the weak formulation, we get for the system (37):

$$\frac{\partial U}{\partial t} + A \frac{\partial U}{\partial x} + B \frac{\partial U}{\partial y} = \Pi_{\mathbf{n}} (L_{\mathbf{n}} U - G_{\mathbf{n}}) \delta_{\partial\Omega}, \quad (40)$$

where $\delta_{\partial\Omega}$ is Dirac distribution on $\partial\Omega$ ⁵ and Π is our boundary projection operator.

Energy balance

Again, we start by considering the energy balance for the weak formulation (40) in the continuous setting. We define the global energy of the solution of (37) by

$$E = \frac{1}{2} \int_{\Omega} V^T U d\Omega, \quad (41)$$

where we take into account the symmetrizability of the system (37). We multiply (40) and integrate over Ω leads to

$$\int_{\Omega} V^T \left(\frac{\partial U}{\partial t} + A \frac{\partial U}{\partial x} + B \frac{\partial U}{\partial y} \right) d\Omega = \int_{\partial\Omega} V^T \Pi_{\mathbf{n}} (L_{\mathbf{n}} U - G_{\mathbf{n}}) d\gamma. \quad (42)$$

We reformulate the left-hand side of (42).

$$\begin{aligned} \int_{\Omega} V^T \left(\frac{\partial U}{\partial t} + A \frac{\partial U}{\partial x} + B \frac{\partial U}{\partial y} \right) d\Omega &= \int_{\Omega} V^T \frac{\partial U}{\partial t} d\Omega + \int_{\Omega} V^T \left(A P^{1/2} \frac{\partial V}{\partial x} + B P^{1/2} \frac{\partial V}{\partial y} \right) d\Omega \\ &= \frac{d}{dt} \int_{\Omega} \frac{1}{2} V^T U d\Omega + \int_{\Omega} V^T \left(A P^{1/2} \frac{\partial V}{\partial x} + B P^{1/2} \frac{\partial V}{\partial y} \right) d\Omega \\ &= \frac{dE}{dt} + \int_{\Omega} V^T \left(A P^{1/2} \frac{\partial V}{\partial x} + B P^{1/2} \frac{\partial V}{\partial y} \right) d\Omega = \frac{dE}{dt} + \int_{\partial\Omega} \frac{1}{2} V^T B_{\mathbf{n}} P^{1/2} V d\gamma \\ &= \frac{dE}{dt} + \int_{\partial\Omega} \frac{1}{2} U^T P^{-1/2} B_{\mathbf{n}} U d\gamma \end{aligned} \quad (43)$$

⁵i.e. for any φ smooth enough, $\langle \delta_{\Omega}, \varphi \rangle = \int_{\partial\Omega} \varphi d\gamma$

Combining (42) and (43), we get the following energy balance.

$$\frac{dE}{dt} + \int_{\partial\Omega} \left[\frac{1}{2} U^T P^{-1/2} B_n U - U^T \Pi_n (L_n U - G_n) \right] d\gamma = 0. \quad (44)$$

For stability, the energy does not increase, i.e. $\frac{dE}{dt} \geq 0$ which is guaranteed if the integral term of the left-hand side of (44) is non-negative. Therefore,

$$\frac{1}{2} U^T P^{-1/2} B_n U - U^T \Pi_n (L_n U - G_n) \geq 0 \quad (45)$$

has to be fulfilled. Inequality (45) imposes the restrictions on the choice of the projection operator Π_n . Switching to the discrete FE setting, the information of (45) will be used to determine Π_n in the following. We will give a concrete example in 5.3.

5 Numerical Simulations

Here, we demonstrate that a pure Galerkin scheme is stable if the boundary procedure is done via the SAT approach. This means we impose the boundary conditions weakly and use an adequate boundary operator as developed in section 4. We focus on several different examples and analyze different properties in this context (error behavior, eigenvalues, etc.). As basis functions, we use Bernstein or Lagrange polynomials of different orders (second to fourth order) on triangular meshes. Nearly, no differences can be seen. The time integration is done via strong stability preserving Runge-Kutta methods of second to fourth order, see [29] for details. We use the same order for space and time discretization.

5.1 Two-Dimensional Scalar Equations

We consider a two-dimensional scalar hyperbolic equation of the form

$$\frac{\partial U}{\partial t} + \mathbf{a}(x, y) \cdot \nabla U = 0, \quad (x, y) \in \Omega, \quad t > 0, \quad (46)$$

where $\mathbf{a} = (a, b)$ is the advection speed and Ω the domain. In this subsection, the initial condition is given by

$$U(x, y, 0) = \begin{cases} e^{-40r^2}, & \text{if } r = \sqrt{(x - x_0)^2 + (y - y_0)^2} < 0.25, \\ 0, & \text{otherwise} \end{cases}$$

It is a small bump with height one located at (x_0, y_0) . We consider homogeneous boundary conditions $G_n \equiv 0$, we do further let the boundary matrix M_n be the identity matrix. The boundary conditions reads $M_n U = U = 0$ for $(x, y) \in \partial\Omega$, $t > 0$ which means that the incoming waves are set to zero.

Linear advection

In our first test, we are considering the linear advection equation in $\Omega = [0, 1]^2$. The advection speed is assumed to be constant. The components of the speed vector \mathbf{a} are given by $(a, b)^T = (1, 0)$ and so the flux is given by $\mathbf{f}(U) = \mathbf{a}U$ with $\mathbf{a} = (1, 0)$. We get inflow / outflow conditions on the left / right boundaries and periodic boundary condition on the horizontal boundaries. In our first test, we use Bernstein polynomials and a fourth order pure Galerkin scheme. The boundary operators are computed using the technique developed in section 4 where the positive eigenvalues are set to zero and the negative ones are used in the construction of Π . For the time discretization we apply strong stability preserving Runge-Kutta (SSPRK) scheme with 5 stages and fourth order with CFL=0.3. We use 1048 triangles. In figure (1), we plot the results from a pure Galerkin scheme with SAT terms at three times. Clearly, the scheme is stable, also at the boundary. Next, we check the real parts of the eigenvalues of our problem using formula (18) for different orders, different

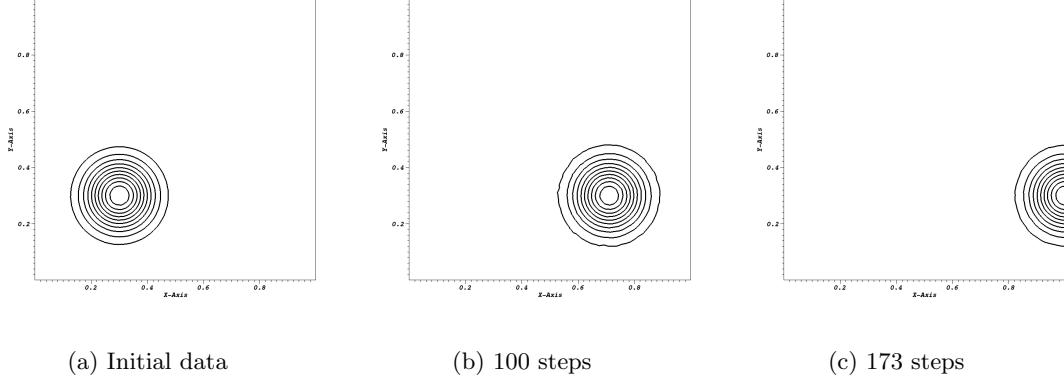


Figure 1: 4-th order scheme in space and time

bases (Bernstein and Lagrange) and different meshes. For the calculation of the eigenvalues of (18), we use a PETSc routine [30, 31] which can calculate up to 500 eigenvalues⁶. Have in mind that in contrast to DG and multi-block FD setting, the mass matrix in the pure Galerkin scheme is not block diagonal. Therefore, we can not split the eigenvalue calculation to each block matrix and have to consider the whole matrix \underline{M} and therefore \underline{Q} . Every coefficient of the numerical approximation belongs to one degree of freedom and we will obtain the same number of eigenvalues as number of DOFs are used. However, for the coefficients which belong to DOFs inside the domain, in all calculations we obtain zero up to machine precision. To get useful results, we decrease the number of elements in the following calculations and provide only the most negative and positive ones in tables 1-3 where we give results with and without the application of the SAT boundary operators.

Table 1: Eigevalue of the operators (25) with and without the boundary operators using $P1/B1$ (41DoFs).

neg. eigen. of $Q + Q^T$	pos. eigen. of $Q + Q^T$	neg. eig. for BT from (25)	pos. eig. for BT from (25)
-0.23173136720035184	0.23173136720035872	-0.31353889462789186	6.0288963880059637 10^{-17}
-0.18392556509888541	0.18392556509888247	-0.25556064666540734	3.8787253053211198 10^{-17}
-0.12500000000000011	0.12500000000000006	-0.23173136720035167	3.0096714657461081 10^{-17}
-6.6074434901127063 10^{-2}	6.6074434901124426 10^{-2}	-0.18484658568172849	2.3845433987475582 10^{-17}
-5.9935299466302876 10^{-2}	5.9935299466301106 10^{-2}	-0.18392556509888475	1.7761773024009382 10^{-17}
-7.2851662848917788 10^{-17}	3.9582511060664642 10^{-17}	-0.12500000000000006	1.2997606751771819 10^{-17}
-4.0169899002806372 10^{-17}	3.4527052584377399 10^{-17}	-0.11811255320367142	9.7095126943382505 10^{-18}
-3.0744506517648380 10^{-17}	2.6741981530660586 10^{-17}	-7.7263266123643440 10^{-2}	9.4396221446379862 10^{-18}
-2.9952903476613825 10^{-17}	2.4022885592771789 10^{-17}	-6.6074434901127105 10^{-2}	9.4396221446379862 10^{-18}
-2.3732437687638515 10^{-17}	1.8552176917490372 10^{-17}	-5.9935299466302945 10^{-2}	6.6811502959265786 10^{-18}
-1.9298861461439164 10^{-17}	1.2937773129407812 10^{-17}	-7.2894055678206064 10^{-17}	5.6739179722400795 10^{-18}

We see from tables 1-3 that the the boundary operator decreases the negative eigenvalues and forces the positive ones to zero (up to machine precision). For third and fourth order, we print only the case using Bernstein polynomials. The applications of Lagrange polynomials lead only to slightly bigger amounts of positive and negative eigenvalues of the $Q + Q^T$ operator (i.e maximum eigenvalue is 0.11713334374388217 for $P3$). However, the results are similar after applying the SAT procedure, we obtain only negative or zero eigenvalues.

We also mention that for higher degrees and more DOFs, we may strengthen the SAT terms to guarantee that the eigenvalues are negative and /or forced to zero and that we do not encounter stability issues because our procedure is too weak. All of our investigations are in accordance with the analysis done in subsection

⁶we have used simple, double and quadruple precision, the results remain the same upto machine precision.

Table 2: Eigevalue of the operators (25) with and without the boundary operators using $B2$ (145DoFs).

neg. eigen. of $Q + Q^T$	pos. eigen. of $Q + Q^T$	neg. eig. for BT from (25)	pos. eig. for BT from (25)
-0.13431144961010608	0.13431144961011104	-0.19242094230739110	2.8085116256406054 10^{-16}
-0.11864982263325710	0.11864982263325606	-0.17455521570137561	2.5390137612709931 10^{-16}
-9.7803643622089528 10^{-2}	9.7803643622090097 10^{-2}	-0.15237284997578737	2.4455634575673296 10^{-16}
-6.1146894711339057 10^{-2}	6.1146894711336615 10^{-2}	-0.13431144961010613	2.2495358302625353 10^{-16}
-5.8451733177756773 10^{-2}	5.8451733177754525 10^{-2}	-0.11864982263325702	2.2016075241289920 10^{-16}
-2.6007668562916055 10^{-2}	2.6007668562916642 10^{-2}	-0.10888636395965785	2.0042786344428149 10^{-16}
-1.6694419035281061 10^{-2}	1.6694419035281158 10^{-2}	-9.7803643622089168 10^{-2}	1.9144133394573818 10^{-16}
-1.0862280759161996 10^{-2}	1.0862280759161619 10^{-2}	-6.925837077729450 10^{-2}	1.8695249872371232 10^{-16}
-9.4054212214267040 10^{-3}	9.4054212214266398 10^{-3}	-6.1146894711339168 10^{-2}	1.8192397731143321 10^{-16}
-2.7616978507002018 10^{-16}	2.8085133451646359 10^{-16}	-5.8451733177756718 10^{-2}	1.7824872125610008 10^{-16}
-2.5756569234550337 10^{-16}	2.5390170077619203 10^{-16}	-3.0332659051060466 10^{-2}	1.7761732673240802 10^{-16}

Table 3: Eigevalue of the operators (25) with and without the boundary operators using $B3$ (313DoFs).

neg. eigen. of $Q + Q^T$	pos. eigen. of $Q + Q^T$	neg. eig. for BT from (25)	pos. eig. for BT from (25)
-9.3745629345829931 10^{-2}	9.3745629345833498 10^{-2}	-0.14166587424610219	2.2109026139735913 10^{-16}
-8.6774440781919981 10^{-2}	8.6774440781920065 10^{-2}	-0.13453327039080706	2.1270302880074533 10^{-16}
-7.7345740375798111 10^{-2}	7.7345740375799499 10^{-2}	-0.12605712972696967	2.0374783880582241 10^{-16}
-5.1492489586678999 10^{-2}	5.1492489586676689 10^{-2}	-9.3745629345830306 10^{-2}	1.9448628993302697 10^{-16}
-5.0243045257037745 10^{-2}	5.0243045257035400 10^{-2}	-9.1241459314117521 10^{-2}	1.9060210717487161 10^{-16}
-3.1541301598810301 10^{-2}	3.1541301598811175 10^{-2}	-8.6774440781919857 10^{-2}	1.8709799567089493 10^{-16}
-2.3206426710231758 10^{-2}	2.3206426710231879 10^{-2}	-7.7345740375798083 10^{-2}	1.8542990724616054 10^{-16}
-1.6529549307273919 10^{-2}	1.6529549307273312 10^{-2}	-5.7862247206398265 10^{-2}	1.7657372661069632 10^{-16}
-1.4887293061954772 10^{-2}	1.4887293061954505 10^{-2}	-5.1492489586678986 10^{-2}	1.6555178664337086 10^{-16}
-4.4006199428851889 10^{-3}	4.4006199428853260 10^{-3}	-5.0243045257037731 10^{-2}	1.6338228753449766 10^{-16}
-3.0050247670574946 10^{-3}	3.0050247670574928 10^{-3}	-3.6266373569196687 10^{-2}	1.6222511624855150 10^{-16}
-2.1187416395799549 10^{-3}	2.1187416395798786 10^{-3}	-3.1541301598810439 10^{-2}	1.6088030692052103 10^{-16}
-1.8525547677998042 10^{-3}	1.8525547677998035 10^{-3}	-2.8789810934290748 10^{-2}	1.5857729151324636 10^{-16}
-2.1398733770045295 10^{-16}	2.2109002259977476 10^{-16}	-2.3206426710231664 10^{-2}	1.5731749183062314 10^{-16}

4.1 and means that that everything is in order and consistent with the theory. All of our calculations demonstrate that a pure Galerkin scheme is stable if a proper boundary procedure is used.

Remark 5.1. Finally, we have done a couple of additional simulations changing both, the domain Ω (circles, pentagons, etc.) and the speed vector including also some horizontal movement. All of our calculations have remained stable if the boundary approach from section 4 was used.

This is in contradiction of a common belief in the research community about continuous Galerkin schemes. But what are the reasons for this belief? In our opinion, one of the major issues is that the exactness of the quadrature rule is chosen too low and without artificial stabilization terms the continuous Galerkin scheme collapses, and the corresponding Q matrix does not become almost skew-symmetric.

Inexactness of the Quadrature Rule

To support our statement, we provide the following example. We consider the same problem as before, but in the Galerkin scheme we lower the accuracy of our quadrature rule so that the mass matrix is not evaluated exactly anymore (up to machine precision). We decrease the CFL number to 0.01 for stability reasons. However, as it is shown in figure 2 the scheme crashes after some time even with this super low CFL number. In pictures 2c, the structure of the bump can still be seen, but, simultaneously, the minimum value is ≈ -2.996 and the maximum value is around 2.7.

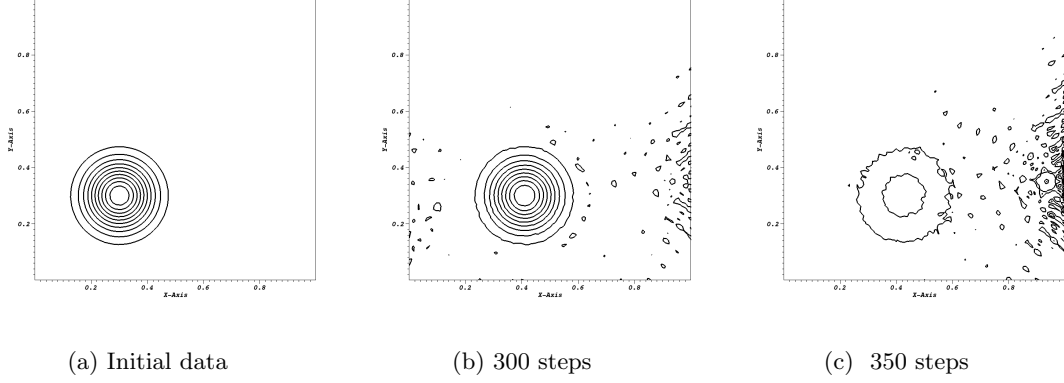


Figure 2: 4-th order scheme in space and time

Additional time steps will lead to a complete crash of the test. Here, again nothing has changed from the calculations before except that the quadrature rule is not exact anymore in the calculation of M , which leads to an erroneous Q matrix, which cannot be stabilized with the SAT boundary treatment.

Linear Rotation

In the next test we are considering an advection problem with variable coefficients. The speed vector has components

$$a = 2\pi y, \quad b = -2\pi x.$$

The initial and boundary conditions are given by

$$U(x, y, 0) = \begin{cases} e^{-40r^2}, & \text{if } r = \sqrt{x^2 - (y - 0.5)^2} < 0.25, \\ 0, & \text{otherwise} \end{cases}$$

$$U = 0, \quad (x, y) \in \partial\Omega, \quad t > 0.$$

The problem is defined on the unit disk $\mathbb{D} = \{(x, y) \in \mathbb{R}^2 \mid \sqrt{x^2 + y^2} < 1\}$. The small bump rotates in the clockwise direction in a circle around zero. In figure 3a the initial state is presented where figure 3b shows the used mesh. We apply an unstructured triangular mesh with 932 triangles. In the second calculation 5382 triangles are used. The time integration is again done via a SSPRK54 scheme with CFL=0.2. A pure continuous Galerkin scheme with Bernstein polynomials is used for the space discretisation. The boundary operator is estimated via the approach presented in 4.1.3. In figure (4), the results are presented after two rotations of the bump. This test again verifies more that our scheme remains stable only through our boundary procedure.

We compute this problem up to ten rotations for different orders. We observe that all of our calculation remain stable both using Lagrange or Bernstein polynomials as can be seen for example in figure 5.

Finally, we analyze the error behavior and calculate the order. In the first step, figure 6 shows the error behaviors for second-fourth order in space and in time after $t = 0.01$ with CFL=0.2. This shows that figure 6 represents mainly the space discretisation, i.e. the pure continuous Galerkin scheme. Here, we see that the space discretization has indeed the desired accuracy order. To include the time integration effects, we determine again the errors, but now after one rotation, see figure 7. We recognize a slight decrease of the order.

The investigation of the decreased order of accuracy is not the main focus of this paper, where we focus on the stability properties of the pure continuous Galerkin scheme.

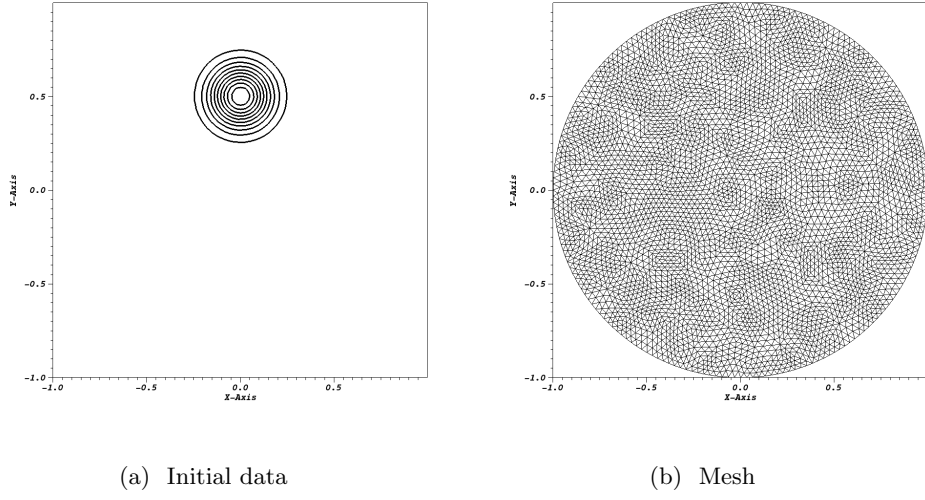


Figure 3: 4-th order scheme in space and time

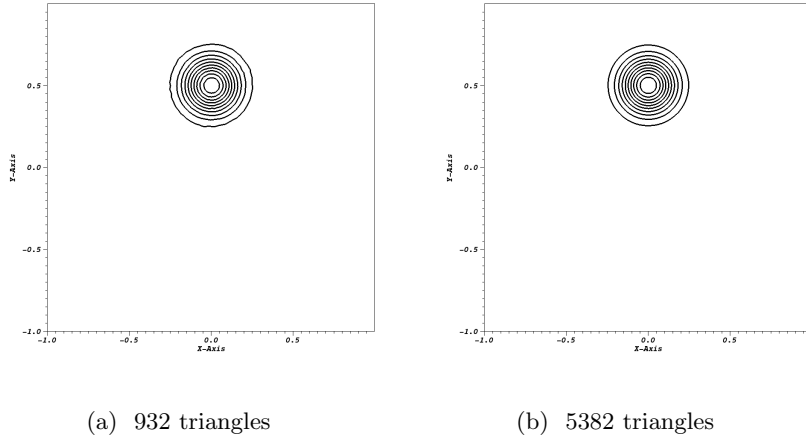


Figure 4: 4-th order scheme in space and time

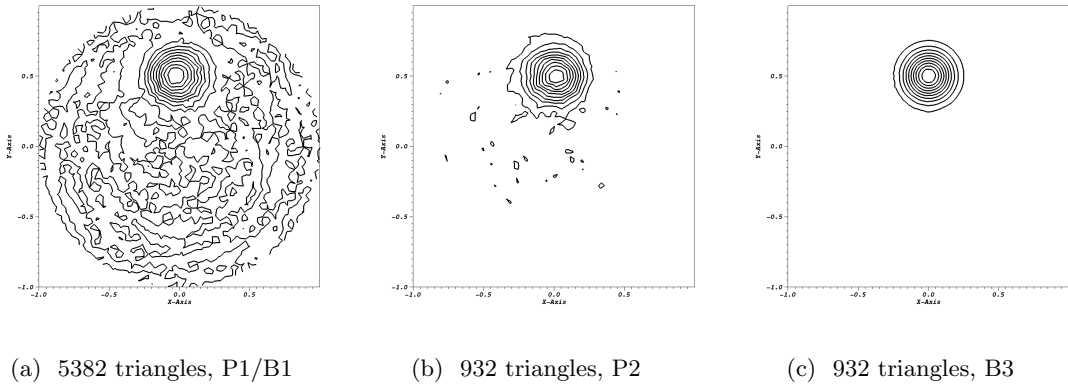


Figure 5: 2,3,4-th order scheme in space and time

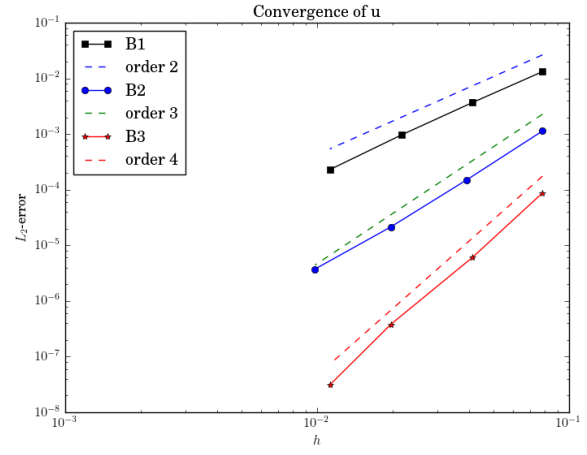
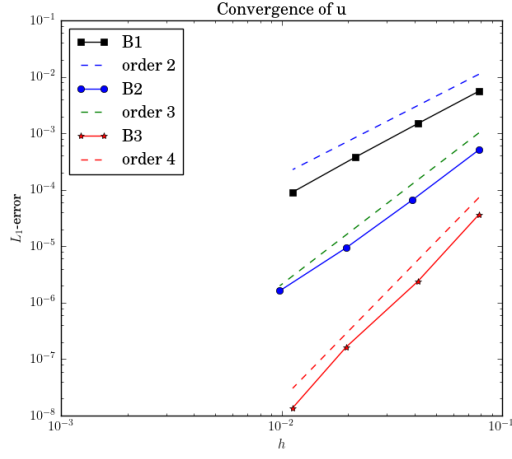


Figure 6: $t = 0.01$, L_1 -error and L_2 -error

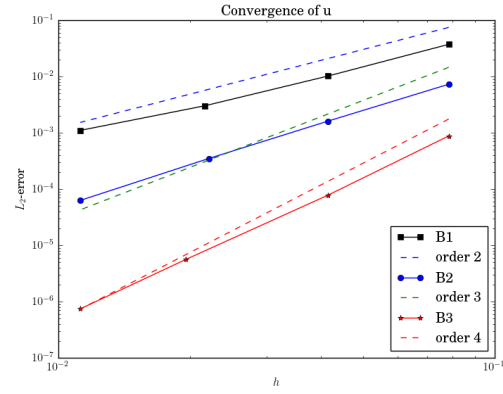
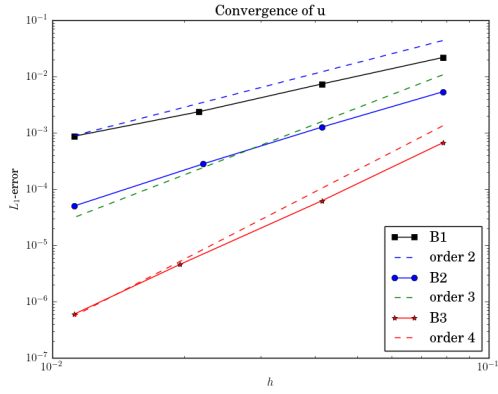


Figure 7: $t = 1$, L_1 -error and L_2 -error

5.2 One-Dimensional Wave Equation

As a first example for systems with non-homogeneous boundary condition, we are considering the linear wave equation

$$u_{tt} - u_{xx} = 0 \quad t > 0, x \in (0, 1),$$

By transformation of variables, we obtain a linear system (26) of first order with coefficient matrix

$$A = \begin{pmatrix} 0 & 1 \\ 1 & 0 \end{pmatrix}.$$

We assume the following sinusoidal boundary conditions:

$$\begin{aligned} x = 0 : \quad & \frac{1}{\sqrt{2}} \begin{pmatrix} 1 & 1 \\ 1 & -1 \end{pmatrix} \begin{pmatrix} \tilde{u} \\ \tilde{v} \end{pmatrix} = \begin{pmatrix} \sin t \\ 0 \end{pmatrix} \\ x = 1 : \quad & \frac{1}{\sqrt{2}} \begin{pmatrix} 1 & 1 \\ 1 & -1 \end{pmatrix} \begin{pmatrix} \tilde{u} \\ \tilde{v} \end{pmatrix} = \begin{pmatrix} 0 \\ \sin t \end{pmatrix} \end{aligned}$$

To determine the boundary operators, we calculate the eigenvalues and the eigenvectors of A following the ideas of subsection 4.1.2. We obtain the eigenvalues $\lambda_{1/2} = \pm 1$ and

$$X = \frac{1}{\sqrt{2}} \begin{pmatrix} 1 & 1 \\ 1 & -1 \end{pmatrix} = X^T$$

where the rows are the eigenvectors. It is $X^T X = \mathbb{I}$. We assume that

$$\Pi_0(M_0(U) - g_0) = \begin{pmatrix} -R_0 & 1 \\ 0 & 0 \end{pmatrix} X^T U - \begin{pmatrix} \sin t \\ 0 \end{pmatrix} \quad \Pi_1(M_1(U) - g_1) = \begin{pmatrix} 0 & 0 \\ 1 & -R_1 \end{pmatrix} X^T U - \begin{pmatrix} 0 \\ \sin t \end{pmatrix}$$

with $|R_0 R_1| < 1$. Described in [23], the problem is well posed in $L^2([0, 1])$. For the time integration, we apply the SSPRK method of third order given in [29] and the space discretization is done via a pure Galerkin scheme of third order using Lagrange polynomials. The CFL condition is set to 0.4. For 100 cells, and $t = 1$ and $t = 2$, and a regular mesh, we have the results displayed in figure 8. We tested it up to $t = 50$ without any stability problems. Under the same terms and conditions, we ran the test again now with a random mesh. Figure 9 demonstrates the results at $t = 2$ with a zoom in in figure 9b to highlight the mesh points. Indeed, no visible difference can be seen between figure 8b and 9a.

5.3 R13 sub-model for Heat Conduction

In our last simulation, we consider the steady R13 sub-model for heat conduction investigated in [32, 33]. It reads

$$\begin{aligned} \operatorname{div} s &= f, \\ \operatorname{grad} \theta + \operatorname{div} \mathbf{R} &= -\frac{s}{\tau}, \\ \frac{1}{2}(\operatorname{grad} s + (\operatorname{grad} s)^T) &= -\frac{\mathbf{R}}{\tau}, \end{aligned} \tag{47}$$

in $\Omega = \{(x, y) | \frac{1}{2} \leq \sqrt{x^2 + y^2} \leq 1\} \in \mathbb{R}^2$. The outer boundary will be denoted by Γ_1 and the inner circle is Γ_0 . The process includes a scalar temperature $\theta \in \mathbb{R}$, a vector values heat flux $s \in \mathbb{R}^2$, and a symmetric tensorial variable \mathbf{R} represented by a symmetric 2×2 matrix. τ is a constant relaxation time.

We set

$$s = (s_x, s_y), \mathbf{R} = \begin{pmatrix} R_{xx} & R_{xy} \\ R_{xy} & R_{yy} \end{pmatrix}$$

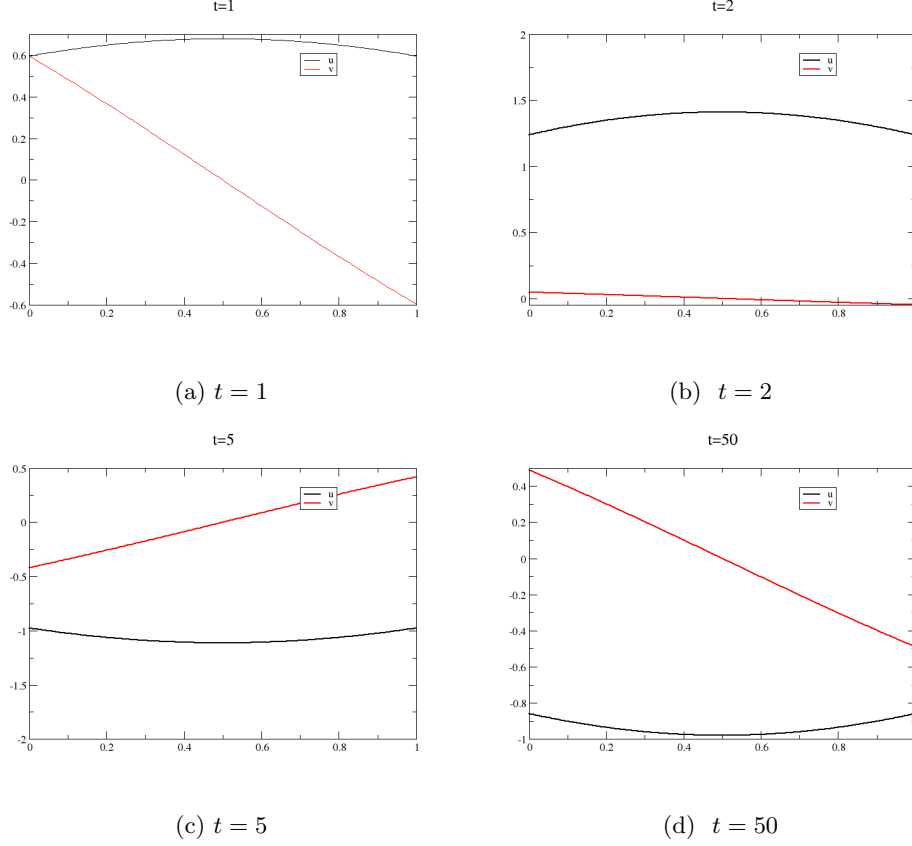


Figure 8: Results for the problem and $t = 1, 2, 5, 50$, 3rd order scheme in space and time

If $U = (\theta, s, \mathbf{R})$ with $\mathbf{R} = (R_{xx}, R_{xy}, R_{yy})$ the system (26) can be rewritten as:

$$AU_x + BU_y = 0.$$

In applications, we will consider the unsteady version of (47)

$$\frac{\partial U}{\partial t} + AU_x + BU_y = 0$$

with boundary conditions that will be detailed in the next part of this section. The aim is to look for a steady solution of this system, and hence to develop a time marching approach. With $\alpha \in \mathbb{R}$, the matrix $\cos \alpha A + \sin \alpha B$ reads

$$A_\alpha = \begin{pmatrix} 0 & \cos \alpha & \sin \alpha & 0 & 0 & 0 \\ \cos \alpha & 0 & 0 & \cos \alpha & \sin \alpha & 0 \\ \sin \alpha & 0 & 0 & 0 & \cos \alpha & \sin \alpha \\ 0 & \cos \alpha & 0 & 0 & 0 & 0 \\ 0 & \frac{\sin \alpha}{2} & \frac{\cos \alpha}{2} & 0 & 0 & 0 \\ 0 & 0 & \sin \alpha & 0 & 0 & 0 \end{pmatrix} \quad (48)$$

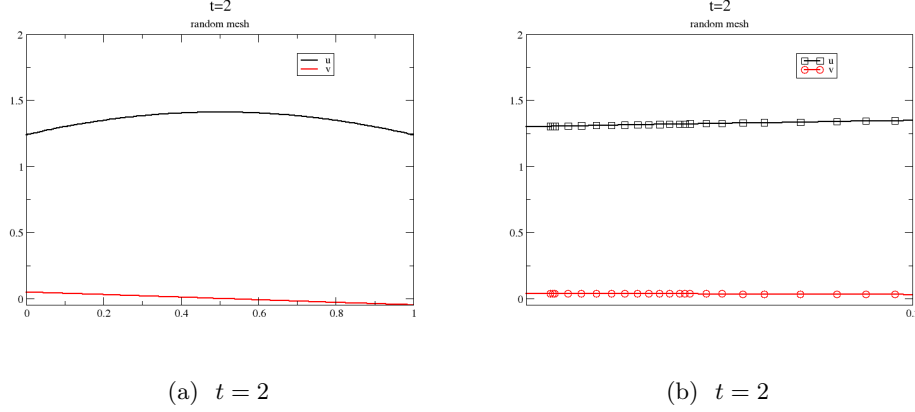


Figure 9: Results for the problem and $t = 2$, irregular mesh, 3rd order scheme in space and time

and we notice that the system (47) is symmetrizable. It is $P = \text{diag}(1, 1, 1, 1, \frac{1}{2}, 1)$ and together, we obtain

$$A_\alpha P = \begin{pmatrix} 0 & \cos \alpha & \sin \alpha & 0 & 0 & 0 \\ \cos \alpha & 0 & 0 & \cos \alpha & \frac{\sin \alpha}{2} & 0 \\ \sin \alpha & 0 & 0 & 0 & \frac{\cos \alpha}{2} & \sin \alpha \\ 0 & \cos \alpha & 0 & 0 & 0 & 0 \\ 0 & \frac{\sin \alpha}{2} & \frac{\cos \alpha}{2} & 0 & 0 & 0 \\ 0 & 0 & \sin \alpha & 0 & 0 & 0 \end{pmatrix} = B_\alpha.$$

B_α is symmetric and to estimate the boundary operator, we need the eigenvalues and eigenvectors of A_n . The eigenvectors are

$$R = \begin{pmatrix} 1 & 1 & 0 & 0 & -1 & -\cos^2 \alpha \\ \sqrt{2} \cos \alpha & -\sqrt{2} \cos \alpha & -\frac{\sqrt{2}}{2} \sin \alpha & \frac{\sqrt{2}}{2} \sin \alpha & 0 & 0 \\ \sqrt{2} \sin \alpha & -\sqrt{2} \sin \alpha & \frac{\sqrt{2}}{2} \cos \alpha & -\frac{\sqrt{2}}{2} \cos \alpha & 0 & 0 \\ \cos^2 \alpha & \cos^2 \alpha & \frac{\sin(2\alpha)}{2} & -\frac{\sin(2\alpha)}{2} & 1 & \cos(2\alpha) \\ \frac{\sin(2\alpha)}{2} & \frac{\sin(2\alpha)}{2} & -\frac{\cos(2\alpha)}{2} & \frac{\cos(2\alpha)}{2} & 0 & \frac{\sin(2\alpha)}{2} \\ \sin^2 \alpha & \sin^2 \alpha & \frac{\sin(2\alpha)}{2} & \frac{\sin(2\alpha)}{2} & 1 & 0 \end{pmatrix} = (R_1, R_2, R_3, R_4, R_5, R_6)$$

associated to the eigenvalues $\lambda = (\sqrt{2}, -\sqrt{2}, \frac{\sqrt{2}}{2}, -\frac{\sqrt{2}}{2}, 0, 0)$. Through P , we can calculate P^{-1} , $P^{1/2}$ and $P^{-1/2}$ without any problems.

Remark 5.2. Since the system is symmetrizable, the eigenvectors are orthogonal for the quadratic form associated to P , i.e. for eigenvectors $r_i \neq r_j$ hold $\langle Pr_i, r_j \rangle = 0$, where $\langle \cdot, \cdot \rangle$ denotes the scalar product.

The boundary conditions

The physical boundary condition follows from Maxwell's kinetic accommodation model. We have

$$\begin{pmatrix} -\alpha\theta + s_x n_x + s_y n_y - \alpha R_{nn} \\ \beta t_x s_x + \beta t_y s_y + t_x n_x R_{xx} + (t_x n_y + t_y n_x) R_{xy} + t_y n_y R_{yy} \end{pmatrix} = M_n U, \quad U = \begin{pmatrix} \theta \\ s_x \\ s_y \\ R_{xx} \\ R_{xy} \\ R_{yy} \end{pmatrix}$$

with normal components $(n_x, n_y) = (\cos \gamma, \sin \gamma)$ and tangential components $(t_x, t_y) = (-\sin \gamma, \cos \gamma)$ where γ is the angle between the x -axis and the outward unit normal on $\partial\Omega$. The accommodation coefficients are given by α and β . We have further $R_{nn} = \cos^2 \gamma R_{xx} + \sin^2 \gamma R_{yy} + 2 \cos \gamma \sin \gamma R_{xy}$ and together

$$M_n = \begin{pmatrix} -\alpha & \cos \gamma & \sin \gamma & -\alpha \cos^2 \gamma & -2\alpha \cos \gamma \sin \gamma & -\alpha \sin^2 \gamma \\ 0 & -\beta \sin \gamma & \beta \cos \gamma & -\cos \gamma \sin \gamma & \cos(2\gamma) & \sin \gamma \cos \gamma \end{pmatrix}.$$

Thanks to this, the boundary conditions on Γ_0 on Γ_1 reads

$$M_n U - \begin{pmatrix} -\alpha \theta_0 \\ -u_x \sin \gamma + u_y \cos \gamma \end{pmatrix} = 0 \text{ on } \Gamma_0, \quad M_n U - \begin{pmatrix} -\alpha \theta_1 \\ 0 \end{pmatrix} = 0 \text{ on } \Gamma_1,$$

where θ_0 and θ_1 are the prescribed temperatures on the cylinders (boundaries of Ω) and u_x, u_y denote the slip velocity. To simplify notations, we introduce G as

$$G_n(x) = \begin{cases} \begin{pmatrix} -\alpha \theta_0 \\ -u_x \sin \gamma + u_y \cos \gamma \end{pmatrix} & \text{if } x \in \Gamma_0, \\ \begin{pmatrix} -\alpha \theta_1 \\ 0 \end{pmatrix} & \text{if } x \in \Gamma_1. \end{cases}$$

We follow the investigation in subsection 4.1.3 and get to the energy balance (44)

$$\int_{\partial\Omega} \left(\frac{1}{2} V^T (A n_x + B n_y) U - V^T \pi M_n U \right) \partial\Omega > - \int_{\partial\Omega} V^T \Pi G_n \partial\Omega.$$

In our practical implementation, we look for Π to get energy stability in the homogeneous case. With (45) and $U = P^{1/2} V$, the condition reads:

$$\frac{1}{2} V^T (A n_x + B n_y) U - V^T \pi M_n U = V^T \left(\left(\frac{1}{2} A_n - \Pi M_n \right) P^{1/2} V \right) > 0. \quad (49)$$

One way to achieve this is to assume that $\frac{1}{2} A_n - \Pi M$ has the same eigenvectors as $\frac{1}{2} A_n$ and that the eigenvalues are positive, i.e. $\Pi M_n - \frac{1}{2} A_n^-$ and ΠM_n and $\frac{1}{2} A_n^-$ have the same eigenvalues⁷. The idea behind is that $(\frac{1}{2} A_n - \Pi M_n) P^{1/2}$ is positive definite. However, this is well-defined under the condition that $M_n P M_n^T$ is invertible. However, we obtain

$$M_n P M_n^T = \begin{pmatrix} 1 + 2\alpha^2 & 0 \\ 0 & \frac{1}{2} + \beta^2 \end{pmatrix}. \quad (50)$$

The matrix is always invertible since its determinant is always bigger than zero. A solution to the problem is $\Pi M_n P M_n^T = R D L P^{1/2} M_n^T$ with $D \leq \frac{1}{2} \Lambda^-$ so $\Pi = R D L P^{1/2} M^T (M P M^T)^{-1}$ with $D \leq \frac{1}{2} \Lambda^-$ and using the transformation with $P^{1/2}$, we obtain:

$$\left(\frac{1}{2} A_n - \pi M_n \right) P^{1/2} V = \lambda P^{1/2} V,$$

i.e.

$$\left(\frac{1}{2} A_n - \lambda I \right) P^{1/2} V = \Pi M_n P^{1/2} V$$

that is

$$\left(\frac{1}{2} A_n - \lambda I \right) P M_n^T (M_n P M_n^T)^{-1} V = \Pi V \quad (51)$$

Using U instead of V in the implementation, we have to multiply Π with $P^{-1/2}$.

⁷Here, we denote again by $-$ the negative eigenvalues.

Remark 5.3. Another way to determine Π , we choose $\delta < 0$ such that $\Pi M_n P^{1/2} - \frac{1}{2} A_n P^{1/2} = \delta Id$, and thus yields

$$\Pi = (\delta P^{-1/2} + \frac{1}{2} A_n) M_n^T (M_n M_n^T)^{-1}.$$

However, this is well-defined under the condition that $M_n M_n^T$ is invertible. We obtain

$$M_n M_n^T = \begin{pmatrix} \frac{1}{4}(4 + 9\alpha^2 - \alpha^2 \cos 4\gamma) & -\frac{1}{4}\alpha \sin 4\gamma \\ -\frac{1}{4}\alpha \sin 4\gamma & \frac{1}{4}(3 + 4\beta^2 + \cos 4\gamma) \end{pmatrix}. \quad (52)$$

The matrix is always invertible since elementary calculations yield to an estimation of the determinate which can be shown to be bigger than 0.5.

Concrete example

We have explained how we estimate the boundary operator in the above equation (51). In the test, we have set the accommodation coefficients $\alpha = 3.0$ and $\beta = -0.5$. The temperature at the boundaries are given by $\theta_0 = 0$ and $\theta_1 = 1$. Further, we have $u_x = 1$ and $u_y = 0$. The relaxation time is set to 0.15. Again, we use a continuous Galerkin scheme together with the above developed boundary procedure. The term δ is set to -2 and the CFL number is 0.1. We are running the problem up to steady state with a RK scheme. In figure 10 we print the mesh and also the result at steady state using a coarse grid. The number of triangles is 400. The problem is elliptic and has to be smooth which cannot be seen in this first picture since the mesh is too coarse.

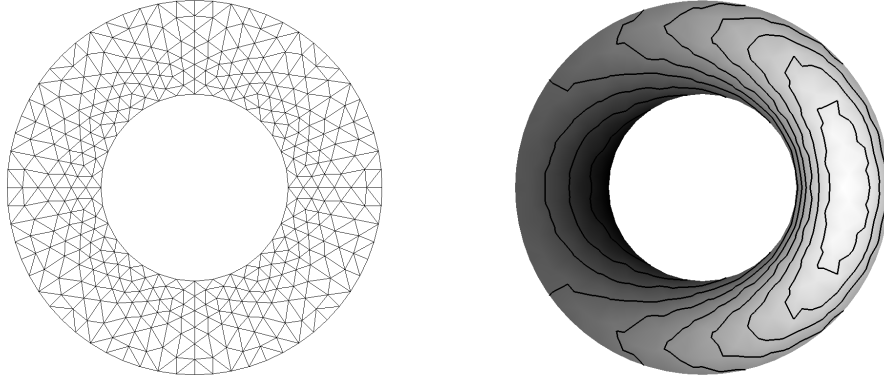


Figure 10: Mesh and steady state ($t = 10$), 3rd order scheme

In the second test, we increase the number of elements in the mesh. Now, we are using 5824 elements and also Bernstein polynomials of second order. The mesh and the result are presented in figure 11. Here, we recognize the smooth behavior and the scheme remains stable only through the above described boundary procedure.

6 Conclusion and Outlook

In this paper, we have demonstrated that a pure continuous Galerkin scheme is stable only through the applied boundary conditions. No further stabilizations terms are needed. This contradicts the common belief about pure continuous Galerkin schemes to be notoriously unstable without additional stabilizations terms. In our approach, the application of the SAT technique is essential where we impose the boundary conditions

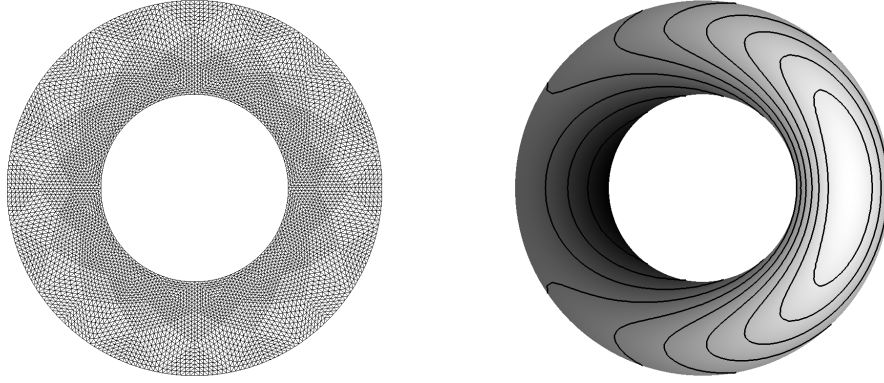


Figure 11: Mesh and steady state ($t = 10$), 3rd order scheme

weakly. Using this approach, we derive a suitable boundary operator from the continuous setting to guarantee that the discrete energy inequality is always fulfilled. We present a recipe how these operators can be constructed, in detail, for scalar two-dimensional problems, one-dimensional systems, and two-dimensional systems. In numerical experiments, we verify our theoretical analysis. Furthermore, in one test, we demonstrate the importance of the used quadrature rule. It has to be exact, if not, the Galerkin scheme suffers from stability issues. If stability can be reached only by enforcing the proper dissipative boundary conditions, there is no free meal: this procedure is very sensitive to any numerical error, like roundoff error or quadrature error.

We think and hope that through our results the common opinion about continuous Galerkin and its application in CFD problems changes, modulo the restriction we have already described. At least this result is interesting from the theoretical point of view, and emphasizes the positive role that the boundary conditions may have. In the companion paper [34], we consider and analyze non-linear (e.g. entropy) stability of continuous Galerkin schemes. Here, the SAT approach will also be important and some approximation for the boundary operators will be developed.

Acknowledgements

P.Ö. has been funded by the the SNF grant (Number 200021_175784) and by the UZH Postdoc grant. This research was initiated by a first visit of JN at UZH, and really started during ST postdoc at UZH. This postdoc was funded by an SNF grant 200021_153604. The Los Alamos unlimited release number is LA-UR-19-32410.

References

- [1] William H Reed and TR Hill. Triangular mesh methods for the neutron transport equation. Technical report, Los Alamos Scientific Lab., N. Mex.(USA), 1973.
- [2] Bernardo Cockburn, George E Karniadakis, and Chi-Wang Shu. *Discontinuous Galerkin methods: theory, computation and applications*, volume 11. Springer Science & Business Media, 2012.
- [3] Jan S Hesthaven and Timothy Warburton. Nodal high-order methods on unstructured grids: I. time-domain solution of maxwell’s equations. *Journal of Computational Physics*, 181(1):186–221, 2002.

- [4] Tianheng Chen and Chi-Wang Shu. Review of entropy stable discontinuous galerkin methods for systems of conservation laws on unstructured simplex meshes1.
- [5] Gregor J Gassner. A skew-symmetric discontinuous Galerkin spectral element discretization and its relation to SBP-SAT finite difference methods. *SIAM Journal on Scientific Computing*, 35(3):A1233–A1253, 2013.
- [6] Mark H Carpenter, Travis C Fisher, Eric J Nielsen, and Steven H Frankel. Entropy stable spectral collocation schemes for the Navier-Stokes equations: Discontinuous interfaces. *SIAM Journal on Scientific Computing*, 36(5):B835–B867, 2014.
- [7] Tianheng Chen and Chi-Wang Shu. Entropy stable high order discontinuous galerkin methods with suitable quadrature rules for hyperbolic conservation laws. *Journal of Computational Physics*, 345:427–461, 2017.
- [8] Jesse Chan. On discretely entropy conservative and entropy stable discontinuous galerkin methods. *Journal of Computational Physics*, 362:346–374, 2018.
- [9] David A Kopriva and Gregor J Gassner. An energy stable discontinuous Galerkin spectral element discretization for variable coefficient advection problems. *SIAM Journal on Scientific Computing*, 36(4):A2076–A2099, 2014.
- [10] Hendrik Ranocha, Philipp Öffner, and Thomas Sonar. Summation-by-parts operators for correction procedure via reconstruction. *Journal of Computational Physics*, 311:299–328, 2016.
- [11] Heinz-Otto Kreiss and Godela Scherer. Finite element and finite difference methods for hyperbolic partial differential equations. *Mathematical aspects of finite elements in partial differential equations*, (33):195–212, 1974.
- [12] David C Del Rey Fernández, Jason E Hicken, and David W Zingg. Review of summation-by-parts operators with simultaneous approximation terms for the numerical solution of partial differential equations. *Computers & Fluids*, 95:171–196, 2014.
- [13] Jason E Hicken, David C Del Rey Fernández, and David W Zingg. Multidimensional summation-by-parts operators: General theory and application to simplex elements. *SIAM Journal on Scientific Computing*, 38(4):A1935–A1958, 2016.
- [14] Magnus Svärd and Jan Nordström. Review of summation-by-parts schemes for initial-boundary-value problems. *Journal of Computational Physics*, 268:17–38, 2014.
- [15] Remi Abgrall, Paola Bacigaluppi, and Svetlana Tokareva. High-order residual distribution scheme for the time-dependent euler equations of fluid dynamics. *Computers & Mathematics with Applications*, 78(2):274–297, 2019.
- [16] Erik Burman, Alexandre Ern, and Miguel A Fernández. Explicit runge–kutta schemes and finite elements with symmetric stabilization for first-order linear pde systems. *SIAM Journal on Numerical Analysis*, 48(6):2019–2042, 2010.
- [17] Erik Burman and Peter Hansbo. Edge stabilization for galerkin approximations of convection–diffusion–reaction problems. *Computer Methods in Applied Mechanics and Engineering*, 193(15-16):1437–1453, 2004.
- [18] William J Layton. Stable galerkin methods for hyperbolic systems. *SIAM Journal on Numerical Analysis*, 20(2):221–233, 1983.
- [19] William J Layton. Stable and unstable numerical boundary conditions for galerkin approximations to hyperbolic systems. In *Hyperbolic Partial Differential Equations*, pages 559–566. Elsevier, 1983.

- [20] Max D Gunzburger. On the stability of galerkin methods for initial-boundary value problems for hyperbolic systems. *Mathematics of Computation*, 31(139):661–675, 1977.
- [21] T.J.R. Hughes, L.P. Franca, and M. Mallet. A new finite element formulation for CFD: I. symmetric forms of the compressible Euler and Navier-Stokes equations and the second law of thermodynamics. *Comp. Meth. Appl. Mech. Engrg.*, 54:223–234, 1986.
- [22] Jan Nordström. Conservative finite difference formulations, variable coefficients, energy estimates and artificial dissipation. *Journal of Scientific Computing*, 29(3):375–404, 2006.
- [23] Jan Nordström. A roadmap to well posed and stable problems in computational physics. *Journal of Scientific Computing*, 71(1):365–385, 2017.
- [24] Mark H Carpenter, David Gottlieb, and Saul Abarbanel. Time-stable boundary conditions for finite-difference schemes solving hyperbolic systems: Methodology and application to high-order compact schemes. *Journal of Computational Physics*, 111(2):220–236, 1994.
- [25] Hendrik Ranocha, Philipp Öffner, and Thomas Sonar. Extended skew-symmetric form for summation-by-parts operators and varying Jacobians. *Journal of Computational Physics*, 342:13–28, 2017.
- [26] Philipp Öffner and Hendrik Ranocha. Error boundedness of discontinuous Galerkin methods with variable coefficients. *Journal of Scientific Computing*, pages 1–36, 2019.
- [27] Jan Nordström and Cristina La Cognata. Energy stable boundary conditions for the nonlinear incompressible navier-stokes equations. *Mathematics of Computation*, 88(316):665–690, 2019.
- [28] Jan Nordström and Frederik Lauren. The spatial operator in the incompressible navier-stokes, oseen and stokes equations. *Computer Methods in Applied Mechanics and Engineering*, in revision, 2019.
- [29] Sigal Gottlieb, David I Ketcheson, and Chi-Wang Shu. *Strong stability preserving Runge-Kutta and multistep time discretizations*. World Scientific, 2011.
- [30] Satish Balay, Shrirang Abhyankar, Mark F. Adams, Jed Brown, Peter Brune, Kris Buschelman, Lisandro Dalcin, Alp Dener, Victor Eijkhout, William D. Gropp, Dmitry Karpeyev, Dinesh Kaushik, Matthew G. Knepley, Dave A. May, Lois Curfman McInnes, Richard Tran Mills, Todd Munson, Karl Rupp, Patrick Sanan, Barry F. Smith, Stefano Zampini, Hong Zhang, and Hong Zhang. PETSc Web page. <https://www.mcs.anl.gov/petsc>, 2019.
- [31] Satish Balay, Shrirang Abhyankar, Mark F. Adams, Jed Brown, Peter Brune, Kris Buschelman, Lisandro Dalcin, Alp Dener, Victor Eijkhout, William D. Gropp, Dmitry Karpeyev, Dinesh Kaushik, Matthew G. Knepley, Dave A. May, Lois Curfman McInnes, Richard Tran Mills, Todd Munson, Karl Rupp, Patrick Sanan, Barry F. Smith, Stefano Zampini, Hong Zhang, and Hong Zhang. PETSc users manual. Technical Report ANL-95/11 - Revision 3.11, Argonne National Laboratory, 2019.
- [32] Manuel Torrilhon. Modeling nonequilibrium gas flow based on moment equations. *Annual review of fluid mechanics*, 48:429–458, 2016.
- [33] Anirudh Rana, Manuel Torrilhon, and Henning Struchtrup. A robust numerical method for the r13 equations of rarefied gas dynamics: Application to lid driven cavity. *Journal of Computational Physics*, 236:169–186, 2013.
- [34] R. Abgrall, J. Nordstrom, P. Öffner, and S. Tokareva. Analysis of the sbp-sat stabilization for finite element methods part ii: Entropy stability.